scientific reports

Check for updates

OPEN

Establishment and characterization of a novel immortalized human aortic valve interstitial cell line

Zihao Wang[1,2], Zhenqi Rao[1,2], Yixuan Wang[1] & Nianguo Dong[1]✉

Primary human aortic valvular interstitial cells (pHAVICs) play crucial roles in maintaining the mechanical structure and microenvironmental homeostasis of aortic valves. Pathologic processes such as inflammation, senescence, apoptosis, and metabolic disorders of valvular interstitial cells often lead to calcified aortic valve disease (CAVD). However, the lack of clinically relevant cellular models has impeded our understanding of CAVD. Here, we immortalized primary HAVICs with SV40 LTA. The iHAVICs (immortalized human aortic valvular interstitial cells) were maintained in a nonsenescent state and still had the potential to be induced into a senescent phenotype. In calcification induction experiments, iHAVICs can be induced to transform into osteogenic phenotypes via different stimuli via different pathways, accompanied by variations in different markers. In conclusion, we established and characterized a novel human immortalized aortic valve interstitial cell line as a practical in vitro experimental tool for the study of aortic valve calcification disease.

Keywords CAVD, Osteogenesis, SV40, Valvular interstitial cell, Cell line

Abbreviations

pHAVICs	Primary human aortic valvular interstitial cells
iHAVICs	Immortalized human aortic valvular interstitial cells
AVICs	Aortic valvular interstitial cells
AVECs	Aortic valvular endothelial cells
CAVD	Calcified aortic valve disease
SV40 LTA	Simian virus 40 large T antigen
qRT-PCR	Quantitative reverse transcription polymerase chain reaction
VDSC	Valve-derived stromal cells
STR	Short tandem repeat
EdU	5-Ethynyl-2′-deoxyuridine
COL1A1	Collagen I Alpha 1
αSMA	α-Smooth muscle actin
Vim	Vimentin
TAGLN	Transgelin
TP53	Tumor protein 53
RB1	Retinoblastoma 1
KEGG	Kyoto Encyclopedia of Genes and Genomes
GO	Gene Ontology
HPi	High-phosphate medium
OM	Osteogenic medium
TNF-α	Tumor necrosis factor alpha
TGF-β	Transforming Growth Factor Beta
IFN	Interferon
iPSC	Induced pluripotent stem cells

Calcified aortic valve disease (CAVD) is an increasing burden on the global health system. According to a multicenter study, there were an estimated 12.6 million cases and approximately 103,000 deaths attributable to CAVD worldwide in 2017[1]. However, without specific medicine for the early stage of CAVD, surgical treatment

[1]Department of Cardiovascular Surgery, Union Hospital, Tongji Medical College, Huazhong University of Science and Technology, 1277 Jiefang Ave., Wuhan 430022, China. [2]Zihao Wang and Zhenqi Rao contributed equally to this work. ✉email: dongnianguo@hotmail.com

is the only choice for patients with severe AV sclerosis or stenosis[2]. As a result, more investigations on the pathogenic mechanisms of CAVD are needed to identify effective therapeutic targets.

Aortic valvular interstitial cells (AVICs) are several clusters of cells along with aortic valvular epithelial cells (AVECs), resident immune cells, and the extracellular matrix that make up the main structure of aortic valve leaflets[3,4]. According to our single-cell RNA sequencing results, the AVICs differentiate into several clusters of valve-derived stromal cells (VDSCs) under multiple pathological conditions and become the major effector cells of valve calcification[5]. To reproduce these pathological processes in vitro, researchers have used diverse stimuli to induce osteogenic differentiation in AVICs obtained from calcified and noncalcified human aortic valves[6–8] or porcine AVICs[9,10]. However, some defects restrict the application of primary aortic valvular interstitial cells (pHAVICs) in scientific research. First, the acquisition of aortic valve specimens is limited by the pathological conditions. During the CAVD sample acquisition, commonly accepted exclusion criteria include bicuspid aortic valves, rheumatic valves, congenital valve disease, moderate-to-severe mineralized valves, and infectious endocarditis-related valves[6]. Second, primary AVICs grow and divide at a slow rate, which hinders the acquisition of enough cells. The most critical drawback of primary HAVICs is that the cell status remains stable during the first few passages but shifts toward apoptosis and senescence during passaging. To establish specific gene knockdown or knockout cell lines for research, it is necessary to establish an immortalized human aortic valve interstitial cell line as the foundation.

The simian virus 40 is a eukaryotic virus discovered in 1960 that has been widely used for cell transformation[11]. The early region of the viral nucleic acid sequence encodes a large T antigen, which plays a central role in cellular immortalization transformation[12]. The LT antigen interacts with various cell cycle-related proteins, such as p53, pRB, and hsc70, to eliminate cell cycle restrictions after being imported into the nucleus, thereby inducing cellular immortalization[13]. SV40 has been applied to establish numerous immortalized cell lines in human, experimental animal, and agricultural crop cells[13–16].

In this study, we transduced SV40-LT into primary human aortic valvular interstitial cells via lentiviral vectors. During successive rounds of cell passaging along with puromycin screening, we finally obtained immortalized HAVICs. Then, we tested the interstitial cell phenotypes, transcriptomic expression, and osteoblast differentiation ability to confirm that iHAVICs are qualified as a cell model for further studies on CAVD.

Materials and methods

Human samples and ethics

Human noncalcified aortic valve leaflets were acquired from a 9-year-old patient diagnosed with dilated cardiomyopathy during heart transplantation surgery at Wuhan Union Hospital. The acquisition of the clinical specimens was performed in accordance with the Declaration of Helsinki, and written permission was obtained from the patient and the legal guardians. This study was approved by the Tongji Medical College Institutional Review Board, Huazhong University of Science and Technology.

Cell culture and immortalization induction

Primary HAVICs were separated from human aortic valves as previously described[6,17]. Briefly, aortic valve leaflets were digested in 1 mg/mL type I collagenase (Biosharp, Hefei, Anhui, China) for 20 min at 37 °C and then gently scraped with a sterile swab to obtain valve endothelial cells on the surface to establish an immortalized endothelial cell line (unpublished research). The remaining tissues were incubated in type I collagenase overnight at 37 °C in 5% CO_2. The digested cells were centrifuged at 1000 rpm for five minutes, and the cell pellet was resuspended and cultured in the medium containing high glucose DMEM (Gibco, Invitrogen, Carlsbad, CA, USA), 10% fetal bovine serum (Gibco) and 1× Penicillin–Streptomycin Solution (Beyotime Biotechnology, Shanghai, China) at 37 °C in 5% CO_2. The fully grown P0 cells were digested with Accutase (Stemcell Technologies, USA) and then passaged to P1 at a 1–2 ratio in 6 cm dishes.

When the primary P1 AVICs were grown to 50% confluence, the cells were infected with the established lentivirus pGMLV-SV40T-PURO (MOI = 80, Genomeditech, Shanghai) with 5 μg/mL polybrene to increase the lentiviral infection efficiency overnight in a 37 °C, 5% CO_2 incubator. The medium was changed on the second day, and the incubation was then continued for another 4 days, with the medium changed every two days. To screen successfully transduced cells, we treated the cells with 1 μg/mL puromycin and incubated them continuously for 96 h. As mentioned above, the cell culture was continued, and routine passages were performed to obtain sufficient cells. The mycoplasma was cleared preventively by Savelt™ (Hanbio, Shanghai, China) before freezing and storage. The immortalized cells were stored at − 80 °C in cell freezing medium (Cellsaving, NCM Biotech, Suzhou, Jiangsu, China).

STR profiling

The live iHAVICs were sent to Procell Life Science & Technology Co., Ltd, Wuhan for STR profiling. DNA was extracted from approximately 1×10^6 iHAVICs with a Microread Genomic DNA Kit. The Microreader™21 ID System was used to amplify 20 STR loci and sex loci. The PCR products were detected with an ABI Genetic Analyzer 3730xl. The results were analyzed via GeneMapperID-X software (Applied Biosystems) and compared with databases such as ATCC, DSMZ, JCRB, and Cellosaurus.

Western blot

Primary and immortalized cells were washed twice with PBS to remove media components and then lysed with a mixture of RIPA buffer containing protease and phosphatase inhibitor cocktails (NCM Biotech, Suzhou, Jiangsu, China), as recommended in the instructions. The protein samples were quantified to 30 μg/lane by a BCA kit (Beyotime Biotechnology, Shanghai, China) and electrophoresed in 4–20% FuturePAGE™s precast gels (ACE Biotechnology, Changzhou, Jiangsu, China) for 45 min. Next, the isolated protein bands were transferred

to PVDF membranes (Millipore, Billerica, MA, USA) via the wet-transfer method. After being blocked for 1 h at room temperature with 5% (wt/vol) skim milk dissolved in TBS-T (1 × TBS with 0.1% Tween-20). The membranes were cropped according to the molecular weights of the proteins and incubated overnight with diluted primary antibodies at 4 °C. After the primary antibody by was washed away with TBS-T, the membranes were incubated at room temperature with the corresponding secondary antibodies. The membranes were exposed after incubation with enhanced chemiluminescence (NCM Biotech, Suzhou, Jiangsu, China). The bands were quantified via Image J 1.55.

RNA-Seq

The cells were harvested and transported to Bioyigene Biotechnology Company in TRIzol reagent and frozen on dry ice. After RNA isolation and quality testing, the samples were sequenced on a DNBSEQ-T7. The results were analyzed with DESeq2 software to identify differentially expressed genes (DEGs), and then Gene Ontology (GO) and Kyoto Encyclopedia of Genes and Genomes (KEGG)[18–20] pathway enrichment analyses were performed. The raw RNA-seq data were uploaded to the Genome Sequence Archive as HRA007843.

RNA extraction and qRT-PCR

The related methods were performed as described previously[21,22]. Briefly, total RNA was extracted with TRIzol reagent (Thermo Fisher) and then reverse transcribed into cDNA. The reverse transcription and quantitative PCR reagents were prepared according to the manufacturer's instructions (Vazyme Biotech, Nanjing, Jiangsu, China). The quantitative RT-PCR was performed on a StepOne Plus thermal cycler (Applied Biosystems) according to the manufacturer's instructions. Detailed information on the primers used in this study is listed in Supplementary Table 1. The results were normalized to GAPDH expression and analyzed in triplicate via the $2^{-\Delta\Delta ct}$ method.

Immunocytochemistry

Primary cells and immortalized cells were grown to 50% confluence on confocal dishes. The cells were fixed in 4% paraformaldehyde (PFA) and permeated with 0.1% Triton X-100. After being blocked with 5% bovine serum albumin (BSA) at 37 °C for 30 min, the cells were incubated with primary antibodies dissolved in 5% BSA at 4 °C overnight. The samples were covered with corresponding secondary antibodies for 1 h at room temperature and treated with antifade mounting medium with DAPI (Beyotime Biotechnology, Shanghai, China). The results were captured with a confocal microscope (Olympus Corporation, Japan).

β-Galactosidase staining

The cells were stained with a senescence β-galactosidase staining kit (Beyotime Biotechnology, Shanghai, China) as previously described[23]. After being fixed with 4% paraformaldehyde for 10 min, the cell samples were incubated with staining working solution at 37 °C overnight. Images were captured with a microscopic imaging system (Micro-shot Technology, Guangzhou, China), and the proportions of cells that stained positively from each sample were analyzed in three random microscopic fields.

EDU

The following components were prepared according to the instructions of the EdU assay kit (Beyotime Biotechnology, Shanghai, China). pHAVICs and iHAVICs (1×10^5)were seeded into confocal dishes and treated with 10 μM EdU solution for 4 h. After being fixed and permeabilized by the reagents mentioned above, the cells were covered with a click additive solution for 30 min. Hoechst 33342 solution was added for 10 min in the dark. The results were observed and captured via a fluorescence microscope (Olympus Corporation, Tokyo, Japan).

Osteogenic induction

The composition of the osteogenic medium used in this study included 10 mM β-glycerophosphate, 50 μM ascorbic acid, and 100 nM dexamethasone, all of which were purchased from Sigma-Aldrich. For phosphate-induced calcification, sodium dihydrogen phosphate and sodium phosphate were formulated as neutral high phosphate solutions containing 3 mM phosphate ions. The cytokines used to test the osteogenic response of iHAVICs included TNF-α (50 ng/mL, Pepretech), TGF-β (20 ng/mL, Pepretech), IFN-α2a (100 ng/mL, MedChemExpress), IFN-beta (100 ng/mL, Proteintech), IFN-γ (100 ng/mL, Pepretech). All the reagents were diluted in antibiotic-free DMEM containing 2% FBS.

Alizarin Red staining

Alizarin Red staining was performed as previously described[24]. The iHAVICs P20 were treated with high phosphate medium for 14 days and then fixed with 4% PFA for 15 min. After being rinsed in distilled water, the cells were stained with an Alizarin Red S staining kit (Science Research Laboratories) for 10 min. After being washed twice with distilled water, calcium depositions were photographed and analyzed, as mentioned above.

Statistical analysis

All the data were analyzed via GraphPad Prism 8 (GraphPad Software, Inc., CA, USA). Data for iHAVICs are biological replicates from different batches of samples from the same strain, and data for pHAVICs are biological replicates from different donors. The values are presented as the means ± standard deviations (SDs). The Shapiro–Wilk test was used to assess the normality of the distribution of the variables. P-values less than 0.05 were considered statistically significant (ns $p > 0.05$, $^{*}p < 0.05$, $^{**}p < 0.01$, $^{***}p < 0.001$, $^{****}p < 0.0001$).

Results

Establishment of novel immortalized human aortic valve interstitial cells (iHAVICs) with interstitial cellular morphology

Primary human aortic valve interstitial cells were acquired and isolated from the recipient's heart during a heart transplantation surgery. After cell culture and cell passage, P1 cells were transduced with the lentiviruses containing the pGMLV-SV40T-PURO vector and screened with puromycin to obtain immortalized HAVICs stably expressing SV40 LTA until P4. The cells were then passaged to P8 to obtain sufficient cells for experiments and storage. (Fig. 1A). Quantitative reverse transcription polymerase chain reaction revealed that the SV40 large T antigen was highly expressed in iHAVICs, whereas pHAVICs did not express the SV40 LTA (Fig. 1B).

To prove the uniqueness of iHAVICs, the cell line was authenticated by analyzing the STR status of 20 microsatellites along with one sexual identification locus and compared with the cell lines in the Cellosaurus database. The existing cell line with the highest matching degree was HS 88.T, which reached 77.42% (Table

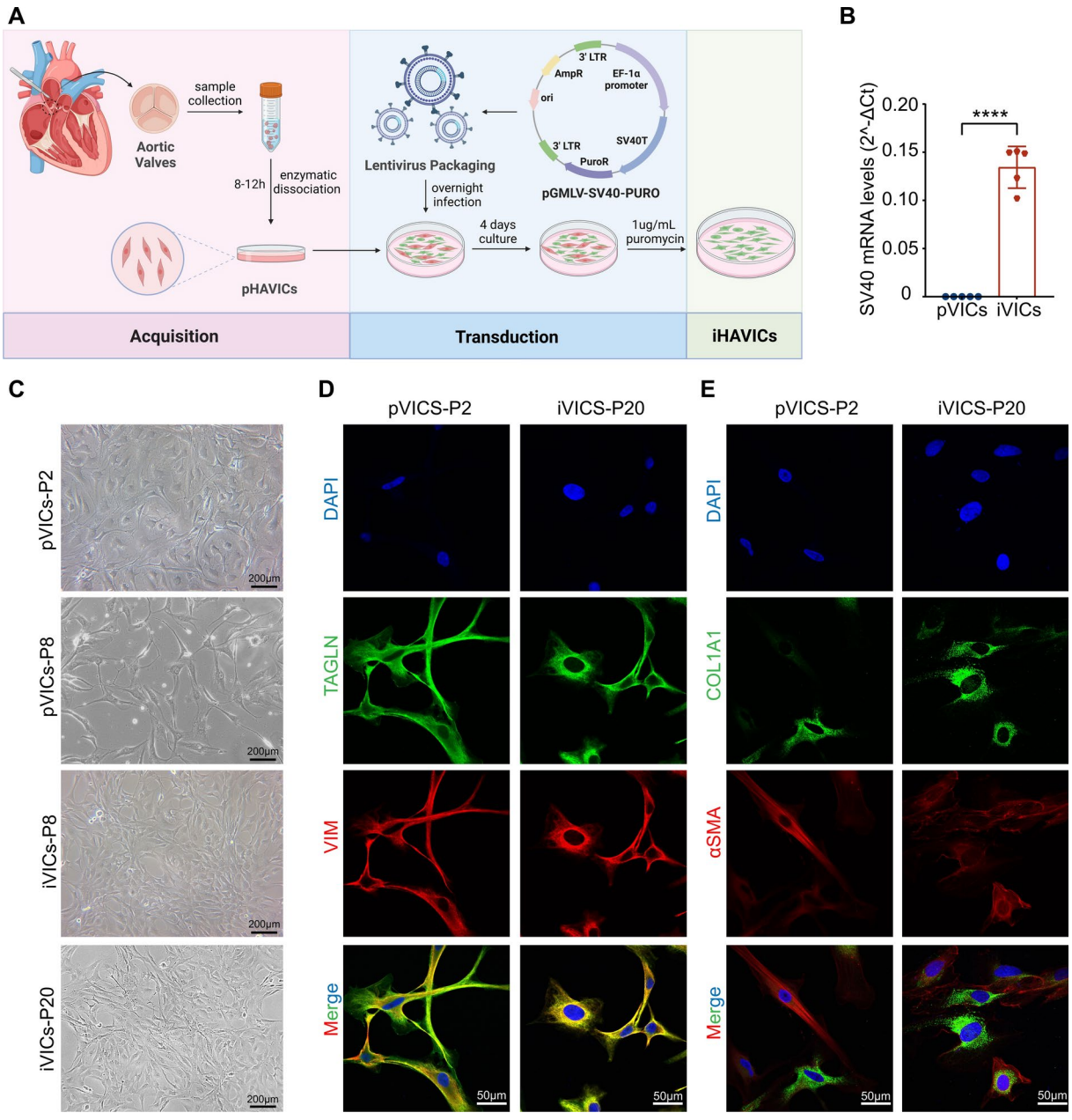

Fig. 1. A novel human immortalized aortic valve interstitial cell line characterized as mesenchymal cells was established. (**A**) Schematic diagram of the process of SV40T transfection via lentiviral vectors leading to the establishment of iHAVICs. The diagram was created in BioRender. Rao, Z. (2025). (**B**) SV40T mRNA expression levels in pHAVICs and iHAVICs (n = 5, $^{****}p < 0.0001$). The data are presented as the mean ± SD values. (**C**) Morphology of P2 and P8 pHAVICs, P8 and P20 iHAVICs. (**D**) Immunofluorescence of mesenchymal cell markers (VIM, TAGLN, COL1A1, and αSMA) in P2 pHAVICs and P20 iHAVICs.

1). According to the cell STR identification criteria established by the International Cell Line Authentication Committee (ICLAC), two cell lines with less than 80% similarity can be considered not significantly correlated. Thus, the iHAVIC is a new type of cell line that is independent of existing cell lines.

Under optical microscope observation, the iHAVICs were generally fusiform or star-shaped and densely interwoven. In areas with low cell numbers, cells extend their branches to establish intercellular connections. Compared with pHAVICs-P2, pHAVICs-P8 showed a smaller number of cells and a more elongated cell morphology, which reflected that the proliferative ability of the primary cells diminished with the increase in the number of passages. In contrast, iHAVICs P8 and P20 had similar cell morphology with larger nuclei and obvious nucleoli, which may be related to vigorous metabolism and active proliferation. (Fig. 1C). With respect to the fluorescence staining of interstitial cell markers (COL1A1, αSMA, Vimentin, TAGLN), both pHAVICs and iHAVICs presented similar staining locations. Vimentin and TAGLN are located at the complete cytoskeleton of both fusiform and star-shaped cells (Fig. 1D). Interestingly, COL1A1 was enriched mostly around the star-shaped cells, whereas αSMA was highly expressed by the fusiform-shaped cells (Fig. 1E). These results suggest that iHAVICs presented similar interstitial cellular morphology as pHAVICs did.

Transcriptomic analysis revealed that immortalization treatment regulated the expression of cell cycle-related genes and cytoskeleton-related genes

To identify the variation in aortic valvular interstitial cells under immortalization conditions, we used RNA sequencing to filter the differentially expressed genes (DEGs) and significantly altered pathways. Compared with those in pHAVICs, 967 genes were upregulated, and 88 genes were downregulated ($padj \leq 0.05$ and $|FoldChange| > 3$), as shown in the volcano plot (Fig. 2B). We screened the top 100 genes on the heatmap according to their log2(fold change) values, and only one gene was downregulated during the immortalization process (Fig. 2A). The top 5 upregulated genes (IL24, CSF2, CCL20, EHF, and IL1B) were used as examples. EHF is a transcription factor that may antagonize p53[25]. The other four genes encode antivirus cytokines and inflammatory cell recruiting factors, which may be related to heterologous genes inserted into the genome.

GO enrichment analysis was performed to assess the cell component (CC), molecular function (MF), and biological process (BP) variations related to immortalization treatment. As shown in Fig. 2C, the cell component domain was enriched with chromosomes, spindle poles, and kinetochores, which are important effector structures in the process of mitosis. With respect to the molecular function domain, microtubule motor activity and microtubule binding were enriched, which may be associated with the depolymerization and reorganization of microtubules during mitosis. Similarly, in the biological process domain, most of the enriched pathways were associated with cell proliferation and antivirus reactions. In addition, we selected 18 genes as markers of AVICs on the basis of previous scRNA-Seq studies[5,26,27]. The fold change values of all these genes did not reach the significance threshold (Fig. 2D). Taken together, these results suggested that immortalization treatment altered mainly mitotic proliferation-related genes and cytoskeleton-related genes but did not alter aortic valvular interstitial cell marker genes.

STR Loci	iHAVIC	Hs 88.T
Amelogenin	X,Y	X
CSF1PO	9,11	11,12
D2S1338	20,20	
D3S1358	15,15	
D5S818	10,11	10,12
D7S820	8,11	8,11
D8S1179	15,16	
D13S317	10,11	10,11
D16S539	11,12	11,13
D18S51	15,16	
D19S433	12,13.2	
D21S11	28,30	
FGA	22,24	
PentaD	9,11	
PentaE	17,23	
TH01	6,9	6,9
TPOX	8,9	8,9
vWA	17,17	15,17
D6S1043	13,14	
D12S391	18,19	
D2S441	12,15	

Table 1. Short tandem repeat test.

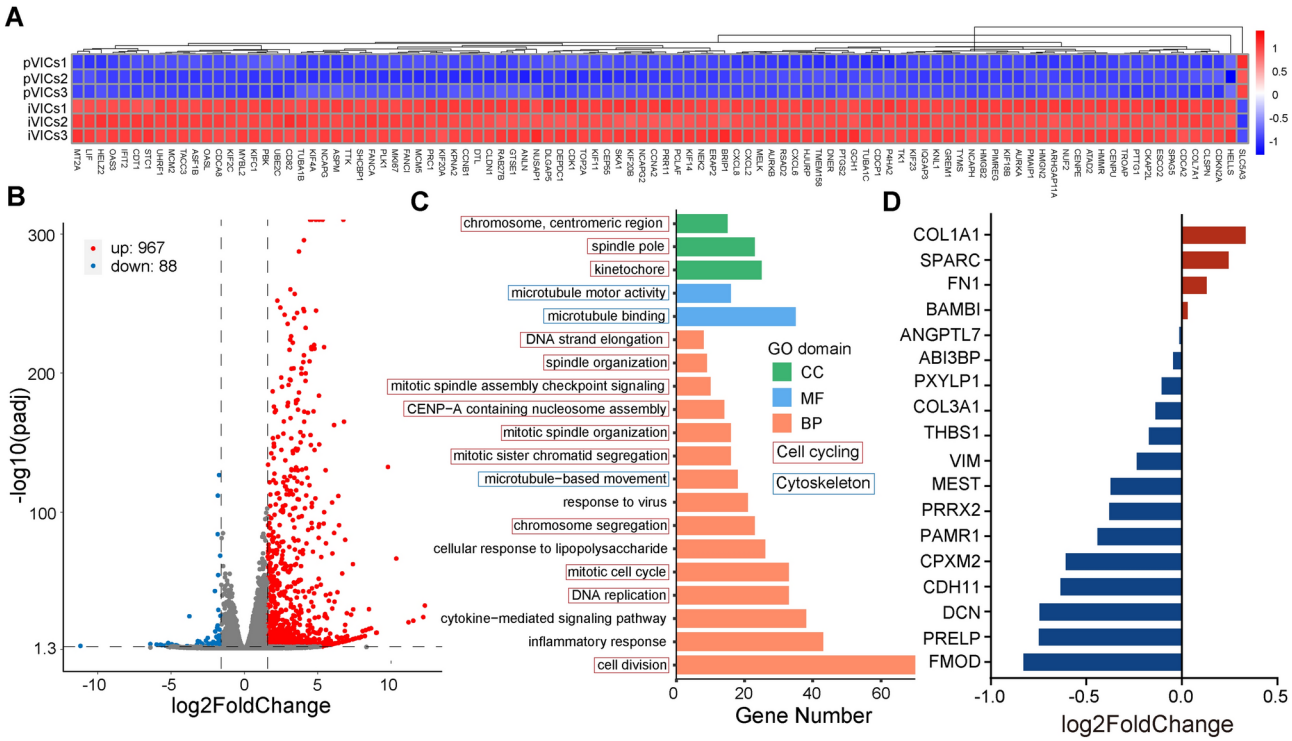

Fig. 2. Bulk RNA-Seq analysis of transcriptome differences between primary and immortalized aortic valve interstitial cells. (**A**) Heatmap representing the top 100 genes differentially expressed between pHAVICs and iHAVICs; (**B**) Volcano plots (padj ≤ 0.05 and |FoldChange|> 3); (**C**) GO enrichment analysis results labeled with orange and blue boxes for the cell cycle and cytoskeleton-related pathways; (**D**) Gene expression of cellular matrix-related markers of aortic valve interstitial cells between pHAVICs and iHAVICs.

Immortalized HAVICs upregulated p53 pathway expression and accumulated greater levels of TP53 and RB1 than primary HAVICs

The mechanism by which viral transfection leads to cell immortalization has been investigated over the past few decades and is briefly summarized in Fig. 3A. Under classical physiological conditions, TP53 monomers are polymerized as tetramers and activated by phosphorylation, thereby binding to DNA to regulate downstream transcription. TP53 tetramers are degraded via the Mdm2-mediated ubiquitin–proteasome pathway, thus maintaining low expression levels in cells[28–33]. After the SV40 large T antigen (LTA) gene sequence is reverse transcribed and integrated into the cell genome, LTAs are stably expressed and distributed in the nucleus. SV40 LTA has a strong affinity for TP53, RB1, and other cell cycle-related proteins and inhibits degradation via ubiquitination to extend the protein half-life. Moreover, the LTA-combined proteins fail to bind DNA and lose their physiological functions[12].

The results of qPCR revealed that the transcript levels of TP53 and RB1 were significantly greater in immortalized cells than in primary cells (Fig. 3B,C). Moreover, transcriptomic data revealed that the majority of TP53 pathway genes were upregulated, whereas only a few apoptosis-related genes were downregulated (BAX, FAS, STEAP3) (Fig. 3D). To detect the protein expression of TP53 and RB1, we prolonged the exposure time of the western blot strips than usual. At this point, only light bands of TP53 and RB1 were shown in the lanes from the primary cell samples, whereas the immortalized cell samples presented much thicker bands (Fig. 3E–G). The fluorescence results corroborated the western blot images revealed that TP53 and RB1 signals were barely detectable in primary cells, whereas immortalized cells presented strong intranuclear fluorescence signals under similar exposure conditions. This difference was not caused by multiple passages (Fig. 3H). Overall, the protein levels of TP53 and RB1 in immortalized cells were significantly greater than those in primary cells.

iHAVICs displayed greater cell viability than pHAVICs

The EdU assay assesses the proliferation ability of cells by embedding fluorescent molecules into the DNA of proliferating cells in terms of the number and intensity of fluorescent signals. As the graph shows, the proportion of EDU-positive cells and the test fluorescence intensity of iHAVICs were much greater than those of pHAVICs (Fig. 4A). For the classical cell replication marker Ki67, the trend in fluorescence intensity was the same as that of the EdU test (Fig. 4B), in which the immortalized cells showed strong proliferative activity. The number of cell proliferating within 144 h for both types of cells is indicated by the line graph (Fig. 4C). Both the rate of proliferation and the final number of cells obtained from the immortalized cells were much greater than those obtained from the primary cells. During the first 36 h after cell seeding, no significant difference was observed between the two types of cells. From 36 h onward, the proliferation of immortalized cells accelerated

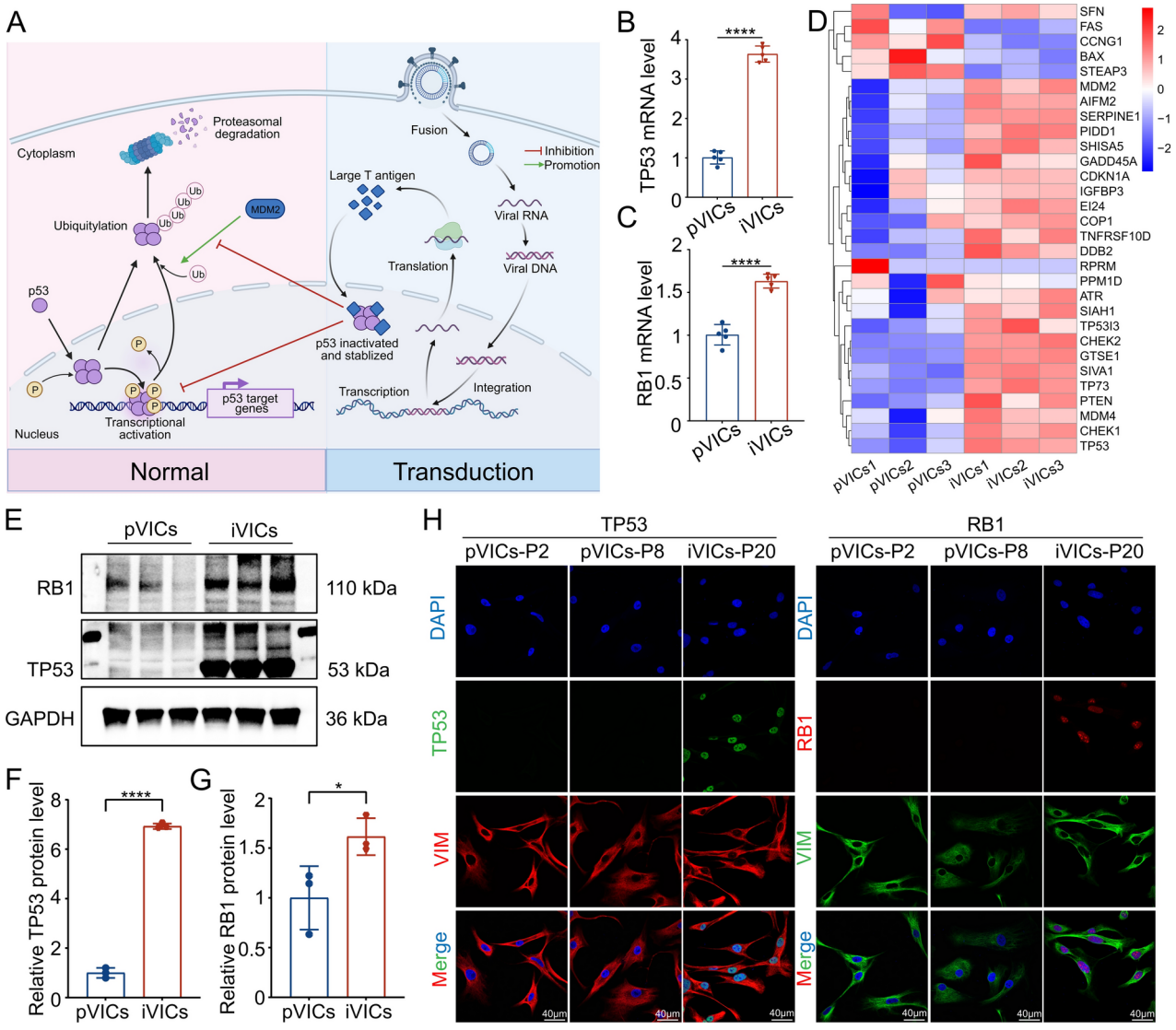

Fig. 3. Differential expression of P53 pathway-related genes in pHAVICs and iHAVICs. (**A**) Schematic diagram of SV40T inhibition of P53 degradation and function. The diagram was created in BioRender. Rao, Z. (2025); (**B**,**C**) qRT-PCR analysis of Tp53 and Rb1 mRNA levels in pHAVICs and iHAVICs (n = 5, $^{****}p < 0.0001$, according to unpaired t- test); (**D**) Heatmap of P53 pathway-related genes from RNA-seq; (**E**–**G**) Western blotting analysis and quantification of RB1 and TP53 expression in pHAVICs and iHAVICs (n = 3, $^{*}p < 0.05$, $^{****}p < 0.0001$, according to unpaired t test); (**H**) Immunofluorescence images demonstrating the expression and localization of TP53 and RB1 in early primary, late primary and immortalized cells.

significantly and slowed to a plateau at 108 h. Ultimately, approximately 1.4 million immortalized cells were harvested per well, which is approximately 1.4 times greater than the number of primary cells. Overall, the iHAVICs proliferated significantly faster and had a higher cell count than the pHAVICs.

To evaluate the senescence state of the cells, we used the β-Gal staining method to treat different generations of primary cells and immortalized cells. As shown in Fig. 4D, the primary cells of P8 presented significantly deeper staining than did the P2 cells. Surprisingly, immortalized P20 cells presented similar staining as primary P2 cells did. These findings indicate that immortalized cells are less likely to age during passaging than primary cells are. However, when immortalized cells were stimulated with an osteogenic induction medium, the degree of staining was significantly greater. No such phenomenon was observed under high phosphate medium stimulation. In summary, iHAVICs are less susceptible to senescence during normal cell passaging and still maintain the potential for senescence under osteogenic stimulation.

iHAVICs maintained relatively stable transcriptome expression during multiple passages

To assess the effects of multiple passages on the transcriptome expression of the cell lines. We compared transcriptome differences between immortalized cells in the tenth generation and immortalized cells that were passed continuously until the 50th generation. As shown in the volcano plot, genes with significant expression

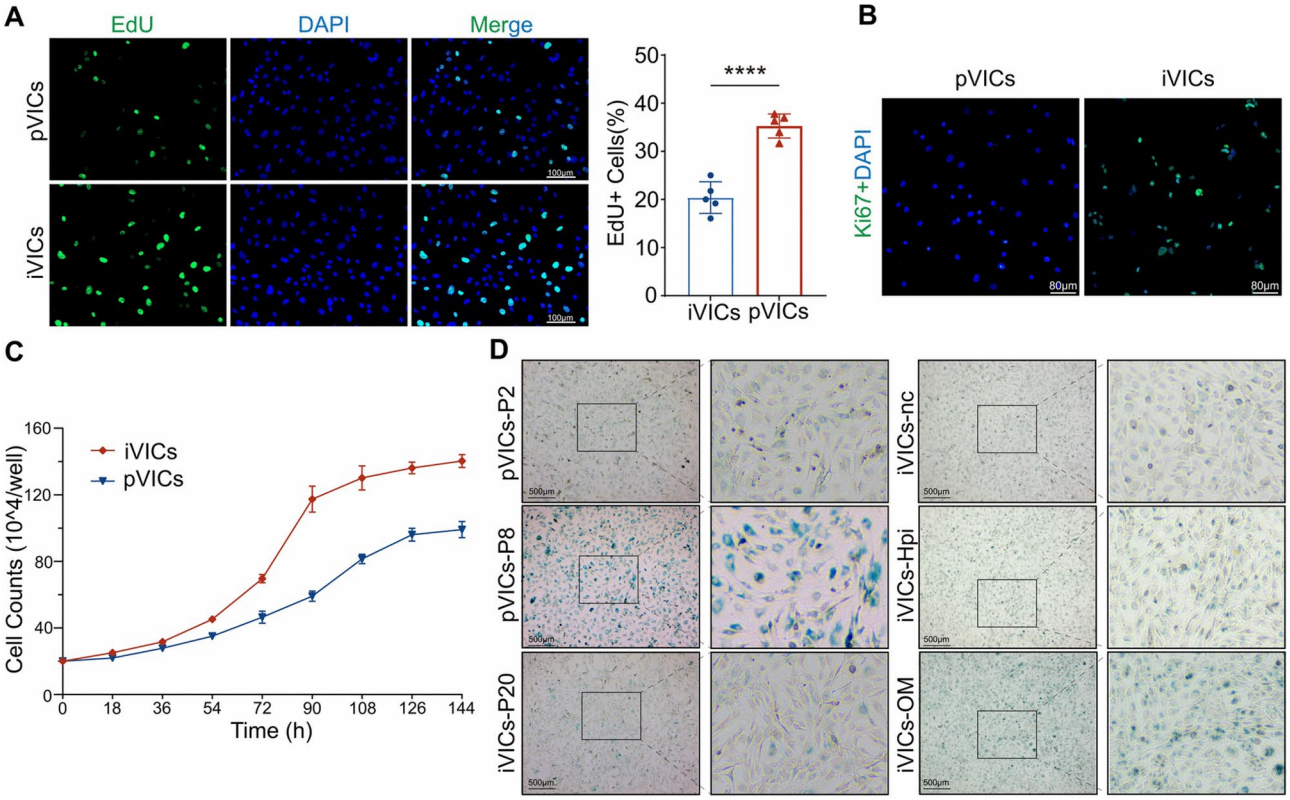

Fig. 4. iHAVICs had greater cell viability than did pHAVICs. (**A**) EdU was used to determine the proportion of cells with active DNA replication for four hours, and statistical analyses were performed in five independent fields (n = 5, $^{****}p < 0.0001$). (**B**) Fluorescence intensity of KI67. (**C**) Primary and immortalized cells cultured in six-well cell culture plates were counted every 18 h. Each scatter represents the average number of cells in three wells. (**D**) β-Gal staining represents the degree of senescence in early-generation primary cells, late-generation primary cells, negative control immortalized cells, and osteogenic-induced immortalized cells (scale bar: 500 μm).

differences were screened at thresholds of |FoldChange| > 2, and padj < 0.05 (Fig. 5A). There were 93 DEGs, of which 54 were upregulated, and 39 were downregulated. The results of the KEGG enrichment analysis of the DEGs are presented in the form of bar charts for both the upregulated and downregulated genes, which revealed that the DEGs were enriched mainly in the inflammatory, mineral metabolism, and lipid metabolism pathways (Fig. 5B,C). However, most pathways were enriched for only 1 or 2 genes, which does not provide strong evidence that successive passages lead to specific changes in cell line function.

With respect to changes in transcriptome expression caused by cell line passage, we are more interested in changes in representative genes related to apoptosis, the cell cycle, mitochondrial function, DNA damage repair, and telomere protection. We selected five representative genes for each aspect and evaluated the alterations in the genes according to their log2FoldChange values (Fig. 5D–H). The log2FoldChange values of these genes varied between − 0.4 and 0.4. Most of the log2FoldChange values were less than 0.1, and we concluded that the expression levels of these genes did not change significantly during successive passages.

Multiple osteogenic inductions lead to diverse osteogenic phenotypes in iHAVICs

Osteogenic phenotypic transformation models of cells are mostly induced by high phosphorus media (containing β-glycerophosphate or inorganic phosphate) or media containing specific cytokines. We used TNFα, TGFβ, inorganic phosphate medium (HPi), OM, and IFN-α, -β, -γ to stimulate immortalized cells and detected changes in the expression of the osteogenic phenotype markers ALPL, BMP2, MSX2, RUNX2, and SP7.

The mRNA levels of markers other than ALPL were increased when the cells were stimulated with TNF-a. Among them, BMP2 was the most significantly upregulated (Fig. 6A). Compared with other markers, SP7 was the most significantly upregulated in response to TGFβ induction (Fig. 6B). When immortalized cells were cultured with inorganic phosphorus medium, the levels of all calcification markers except for SP7 were significantly increased (Fig. 6C). In response to stimulation by type I interferons, BMP2, MSX2, and RUNX2 are more responsive. In response to IFN-γ stimulation, ALPL was significantly upregulated, whereas RUNX2 showed the opposite trend. In response to OM stimulation, ALPL and RUNX2 were significantly upregulated, and interestingly, all three interferons inhibited OM-induced ALPL upregulation to some extent. OM-induced RUNX2 upregulation was enhanced by type I interferons, whereas IFNγ very significantly abolished OM-induced RUNX2 upregulation (Fig. 6D–F). Alizarin red staining confirmed the inorganic phosphorus-induced

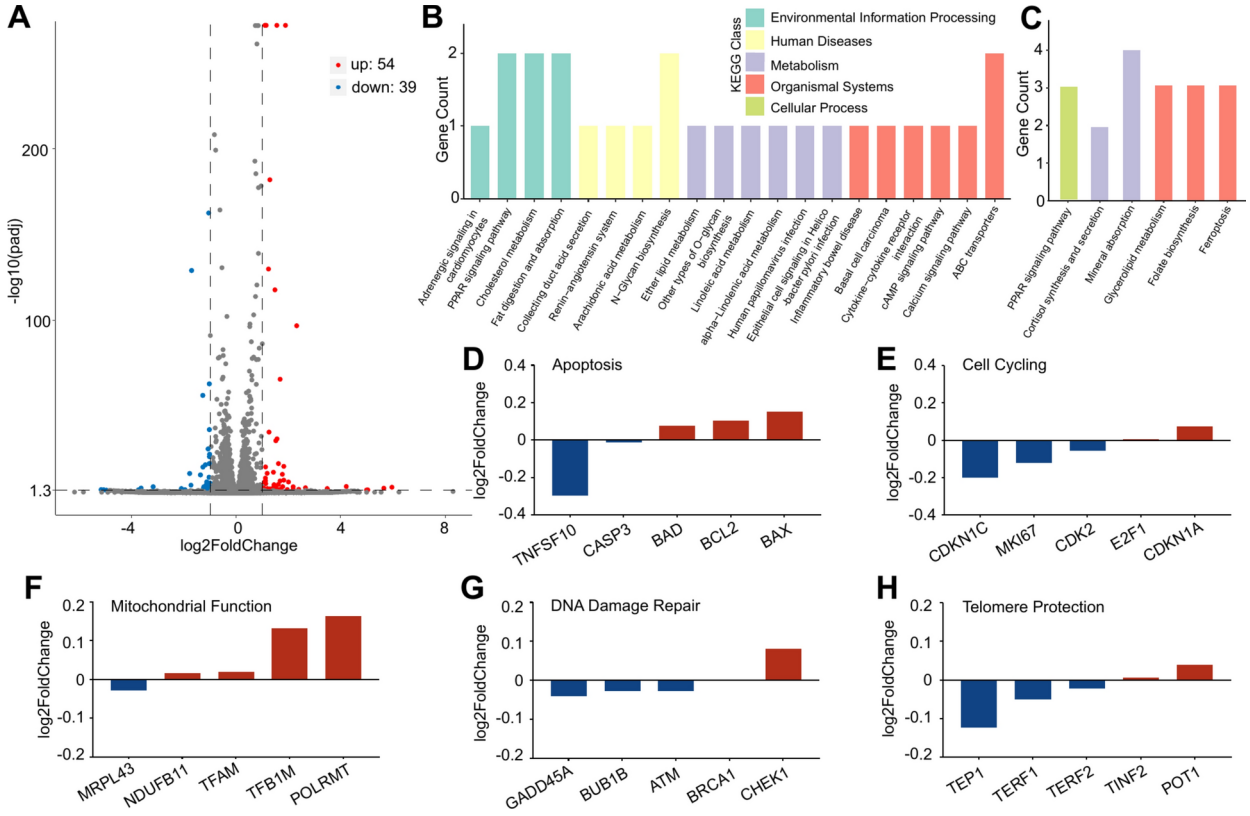

Fig. 5. RNA-seq revealed that iHAVICs maintained relatively stable transcript expression after multiple passages. (**A**) Volcano plot showing transcriptional differences between P10 and P50 iHAVICs (|fold change|> 2, padj < 0.05). (**B**,**C**) KEGG enrichment analysis and the number of enriched genes for selected pathways. (**D**–**H**) Differential expression of representative genes involved in apoptosis, the cell cycle, mitochondrial function, DNA damage, and telomere protection between P10 and P50 iHAVICs.

deposition of calcified nodules in immortalized cells (Fig. 6G). The protein levels of ALPL and RUNX2 increased daily over a 5-day OM induction time course.

RNA-seq suggested the centrality of inflammatory response-related molecules in the osteogenic transformation of immortalized cells

We stimulated cells with osteogenic induction medium to explore changes in the transcriptome of immortalized cells in response to classical osteogenic induction. As shown in the volcano plot, a total of 177 genes were upregulated, and 220 genes were downregulated 2 days after OM stimulation (Fig. 7A). The top ten upward and downward genes are shown in Fig. 7B. We used the STRING database to analyze the interconnections of the proteins corresponding to the differentially expressed genes and to map the protein–protein interaction (PPI) network. IL6 clearly has the highest number of associated proteins and is in the core position. CXCL8, VEGFA, and IL1B are also important in the PPI network (Fig. 7D). The DEGs were subjected to GO enrichment analysis, and in the CC domain, the DEGs were enriched in the extracellular matrix and collagen-related gene sets. According to the results of the molecular function (MF) and biological process (BP) analyses, the pathways enriched with the DEGs were mainly inflammatory and cytokine-related pathways and pathways associated with extracellular matrix remodeling (Fig. 7E).

Discussion

In this study, we established and characterized a novel human immortalized aortic valve interstitial cell line for the in vitro study of aortic valve calcification disease. Although most of the previous articles on aortic valve calcification have used primary aortic valve cells from different patients as an in vitro research tool, extracting primary aortic valve interstitial cells from human aortic valves and culturing them for expansion is a difficult process. The extraction process may be accompanied by contamination, a long passaging period, a small cell volume, and individual variation, all of which affect in vitro experiments. Recently reported induced pluripotent stem cells (iPSCs) partially compensate for the shortcomings of primary cells, but the long induction and differentiation process of iPSCs and the high cost of the cytokines and cell-sorting reagents used limit the wide application of iPSCs[34,35].

Here, we constructed a human immortalized aortic valve interstitial cell line via the lentiviral transfection of SV40T. This cell line is characterized by the significant accumulation of RB1 and TP53 in the nucleus, along

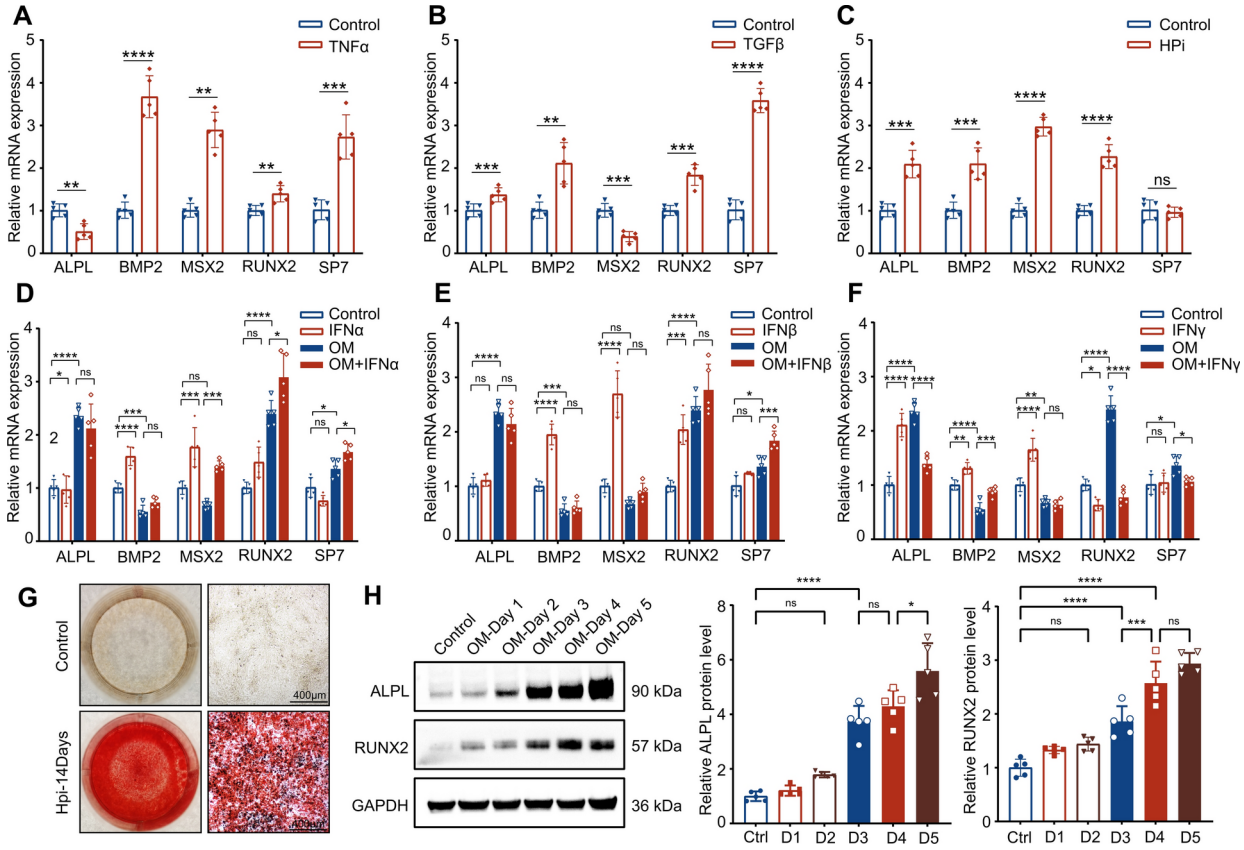

Fig. 6. iHAVICs presented diverse osteogenic phenotypes in response to multiple stimuli (n = 5, ns $p > 0.05$, $^{*}p < 0.05$, $^{**}p < 0.01$, $^{***}p < 0.001$, $^{****}p < 0.0001$). (**A**–**C**) mRNA levels of osteogenic transformation markers (Alpl, Bmp2, Msx2, Runx2, and Sp7) after treatment with TNF-α, TGF-β, or high-phosphate medium; (**D**–**F**) mRNA levels of osteogenic transformation markers (Alpl, Bmp2, Msx2, Runx2, and Sp7) after treatment with interferon-α, -β, or -γ alone or in combination with osteogenic medium. (**G**) Calcium deposition in iHAVICs after 14 days of high-phosphate medium stimulation. (**H**) Western blot analysis and quantification of ALPL and RUNX2 protein expression after 5 days of continuous induction with osteogenic medium.

with stable expression of mesenchymal cell markers (α-SMA, COL1A1, Vimentin, and SM22). Previous studies have suggested that the principle of cellular immortalization by SV40T is closely related to TP53. SV40T binds tightly to TP53, inhibiting its ability to regulate the cell cycle and sparing it from degradation by proteases[36,37]. This finding is consistent with our observation of TP53 nuclear accumulation.

Transcriptome sequencing revealed that the transcript levels of cell cycle-related genes and cytoskeleton-related genes were significantly increased in immortalized cells compared with those in primary aortic valve interstitial cells, suggesting that immortalized cells may exhibit increased cell proliferation activity. We subsequently demonstrated this through the EdU assay, Ki67 assay, and cell counting assay. In addition, we demonstrated via transcriptome sequencing that the immortalized cell lines did not exhibit significant differences in transcript levels after multiple passages and that the representative genes associated with apoptosis, proliferation, mitochondria, DNA damage repair, and telomeres did not undergo significant differential transcriptional changes.

Osteogenic transformation of cells is a pathologic process induced by multiple factors (disturbances in calcium and phosphorus metabolism, high-fat environment, inflammatory stimuli, etc.). We tested the potential of novel human immortalized aortic valve interstitial cells as an in vitro study of calcification, with the aim of informing users of iHAVICs in different calcification environments and thus selecting more precise calcification markers and timing of interventions in different calcification study contexts. Cellular osteogenic-like transformation is closely linked to a high-phosphorus environment[38]. Classical OM successfully increased the protein levels of the calcification markers ALPL and RUNX2 in immortalized cells, whereas treatment with inorganic high-phosphorus medium for 14 days resulted in the production of visible calcium nodules. Previous studies have shown that aortic valve calcification is closely related to inflammation, in which cytokines such as TNFα, TGFβ, type I interferon, and IFNγ may play important roles[39–41]. Notably, when we immortalized cells were stimulated with different inflammatory factors, the changes in the expression of calcification markers varied. TNFα stimulated the upregulation of BMP2, RUNX2, MSX, and SP7; TGFβ had a more pronounced inducing effect on BMP2, RUNX2, and SP7; and type I interferon stimulated the up-regulation of BMP2, RUNX2, and MSX and was synergistic with OM induction, resulting in a synergistic effect. However, IFNγ downregulated the

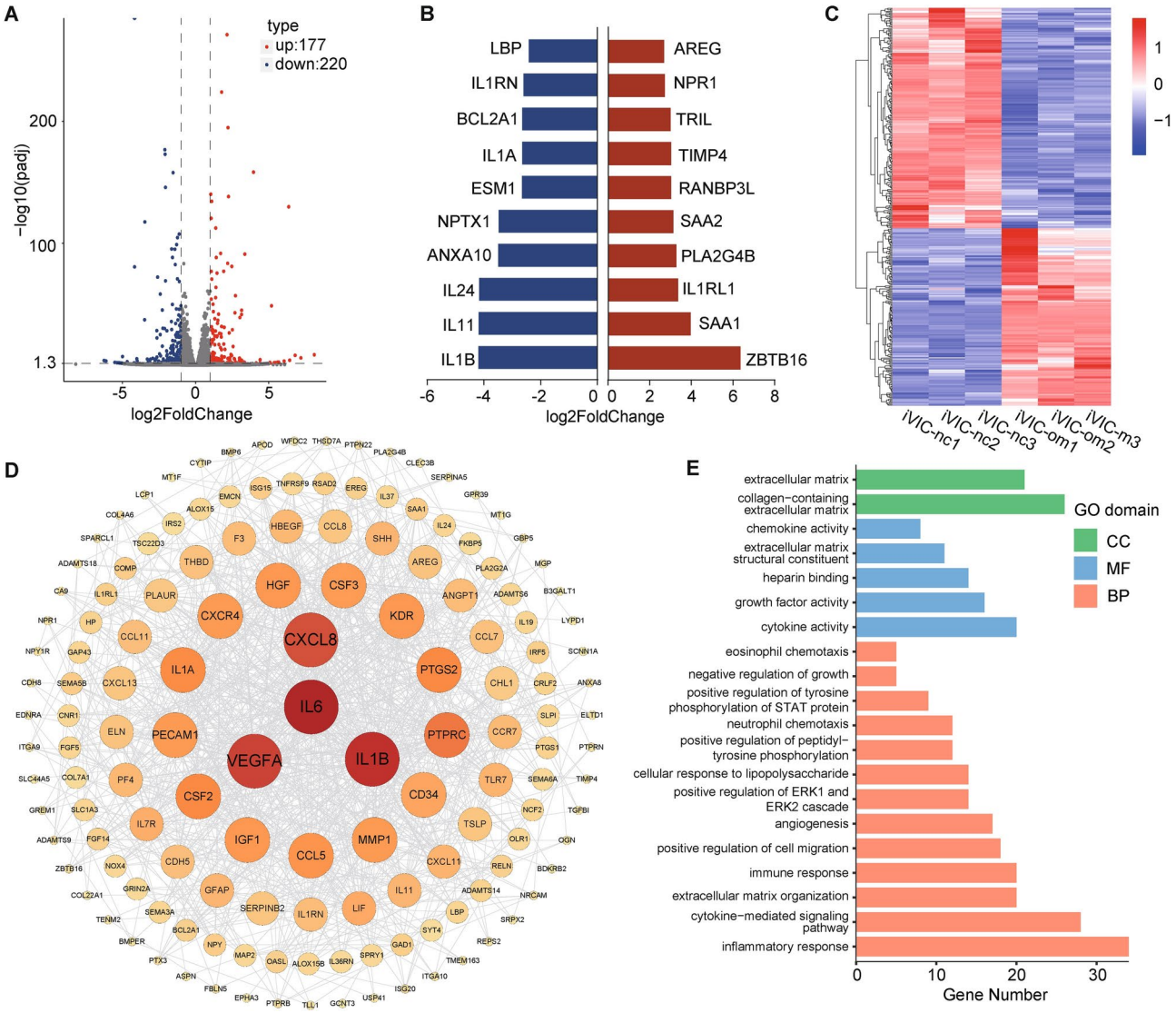

Fig. 7. RNA-seq suggested the centrality of inflammatory response-related molecules in the osteogenic transformation of immortalized cells. (**A**) Volcano plot showing transcriptional differences in iHAVICs between the negative control group and the OM induction group (|fold change|> 2, padj < 0.05); (**B**) Top 10 upregulated genes and downregulated genes; (**C**) Clustering heatmap of differentially expressed genes; (**D**) Protein–protein interaction networks (PPIs) of differentially expressed genes; (**E**) GO enrichment analysis of differentially expressed genes.

expression of calcification markers. The above descriptive findings suggested that when investigating the effect of target genes of different pathways on the pathogenesis of CAVD in the immortalized in vitro model, attention should be paid to the selection of osteogenic markers that are more sensitive to the relevant calcification stimuli, so as to more accurately respond to the pathological progression of osteogenic transformation.

In addition, we examined the transcriptomic changes in novel immortalized aortic valve interstitial cells under OM osteogenesis-inducing stimulation, and GO enrichment analyses suggested significant changes in inflammatory pathways and extracellular matrix remodeling pathways in OM-stimulated immortalized cell lines. Protein interaction analysis suggested that IL6, CXCL8, VEGFA, and IL1B were at the core of the interaction network of DEGs. Notably, inflammation-related molecules were present in the top ten upregulated and downregulated genes. This may be related to dexamethasone stimulation in OM. According to the literature, dexamethasone induces the osteogenic transformation of fibroblasts[42]; however, it should not be ignored that dexamethasone is also a potent anti-inflammatory hormone that has the potential to inhibit the expression of inflammatory genes while inducing osteogenic transformation. These findings suggest that appropriate interventions and markers should be selected according to the different calcification backgrounds.

This study comprehensively characterized SV40T-induced immortalized human aortic valve interstitial cells and explored the application of this cell line in valve calcification studies. However, SV40T virus transfection and other immortalization induction methods such as hTERT virus induction can significantly elevate the

expression of cell cycle-related genes, enabling the primary cells to pass on multiple times. This up-regulation of cell cycle genes due to viral intervention has the potential to alter the molecular mechanisms of calcification in the in vitro model, thereby increasing the discrepancy between in vivo and in vitro results. Secondly, iHAVICs, like pHAVICs, may be potentially disturbed by donor effects. HAVICs derived from patients with dilated cardiomyopathy may have mutations in genes such as ACTC1, MYH7, TNNT2, TNNI3, TPM1, etc., which play important roles in dilated cardiomyopathy. The effect of these potential mutations on aortic valve calcification is unpredictable. Moreover, this study did not explore the mechanism of SV40T-induced cell immortalization in more detail, nor did it compare the differences between immortalized cells and iPSCs. In the future, more in vitro studies may be needed to characterize the different features of primary cells, iPSCs, and immortalized cells.

Conclusion

We established and characterized a novel human immortalized aortic valve interstitial cell line. Various results suggest that the novel immortalized human interstitial cell line is a practical in vitro experimental tool for the study of aortic valve calcification disease.

Data availability

The authors confirm that the data is provided within the manuscript or supplementary information files. The datasets generated during the current study are available in the Genome Sequence Archive repository (HRA007843).

Received: 4 September 2024; Accepted: 7 January 2025
Published online: 29 March 2025

References

1. Yadgir, S. et al. Global, regional, and national burden of calcific aortic valve and degenerative mitral valve diseases, 1990–2017. *Circulation* **141**, 1670–1680. https://doi.org/10.1161/CIRCULATIONAHA.119.043391 (2020).
2. Bartoli-Leonard, F., Zimmer, J. & Aikawa, E. Innate and adaptive immunity: the understudied driving force of heart valve disease. *Cardiovasc. Res.* **117**, 2506–2524. https://doi.org/10.1093/cvr/cvab273 (2021).
3. Wu, B. et al. Developmental mechanisms of aortic valve malformation and disease. *Annu. Rev. Physiol.* **79**, 21–41. https://doi.org/10.1146/annurev-physiol-022516-034001 (2017).
4. Wang, H., Leinwand, L. A. & Anseth, K. S. Cardiac valve cells and their microenvironment—insights from in vitro studies. *Nat. Rev. Cardiol.* **11**, 715–727. https://doi.org/10.1038/nrcardio.2014.162 (2014).
5. Xu, K. et al. Cell-type transcriptome atlas of human aortic valves reveal cell heterogeneity and endothelial to mesenchymal transition involved in calcific aortic valve disease. *Arterioscler. Thromb. Vasc. Biol.* **40**, 2910–2921. https://doi.org/10.1161/ATVBAHA.120.314789 (2020).
6. Wang, Y. et al. DUSP26 induces aortic valve calcification by antagonizing MDM2-mediated ubiquitination of DPP4 in human valvular interstitial cells. *Eur. Heart J.* **42**, 2935–2951. https://doi.org/10.1093/eurheartj/ehab316 (2021).
7. Peng, X. et al. 4-Octyl itaconate suppresses the osteogenic response in aortic valvular interstitial cells via the Nrf2 pathway and alleviates aortic stenosis in mice with direct wire injury. *Free Radic. Biol. Med.* **188**, 404–418. https://doi.org/10.1016/j.freeradbiomed.2022.06.246 (2022).
8. Xu, R., Huang, Y., Zhu, D. & Guo, J. Iron promotes Slc7a11-deficient valvular interstitial cell osteogenic differentiation: A possible mechanism by which ferroptosis participates in intraleaflet hemorrhage-induced calcification. *Free Radic. Biol. Med.* **184**, 158–169. https://doi.org/10.1016/j.freeradbiomed.2022.03.013 (2022).
9. Majumdar, U. et al. Nitric oxide prevents aortic valve calcification by S-nitrosylation of USP9X to activate NOTCH signaling. *Sci. Adv.* https://doi.org/10.1126/sciadv.abe3706 (2021).
10. Liu, H. et al. Celastrol alleviates aortic valve calcification via inhibition of NADPH oxidase 2 in valvular interstitial cells. *JACC Basic Transl. Sci.* **5**, 35–49. https://doi.org/10.1016/j.jacbts.2019.10.004 (2020).
11. Sweet, B. H. & Hilleman, M. R. The vacuolating virus, S.V. 40. *Proc. Soc. Exp. Biol. Med.* **105**, 420–427. https://doi.org/10.3181/00379727-105-26128 (1960).
12. Cheng, J., DeCaprio, J. A., Fluck, M. M. & Schaffhausen, B. S. Cellular transformation by Simian Virus 40 and Murine Polyoma Virus T antigens. *Semin. Cancer Biol.* **19**, 218–228. https://doi.org/10.1016/j.semcancer.2009.03.002 (2009).
13. Chen, Y. et al. Characterization and establishment of an immortalized rabbit melanocyte cell line using the SV40 large T antigen. *Int. J. Mol. Sci.* https://doi.org/10.3390/ijms20194874 (2019).
14. Jiang, H. et al. Establishment and characterization of an immortalized epicardial cell line. *J. Cell Mol. Med.* https://doi.org/10.1111/jcmm.16496 (2021).
15. Yu, Q. et al. Establishment and characterization of an immortalized human giant congenital melanocytic nevi cell line. *Pigment Cell Melanoma Res.* **35**, 356–368. https://doi.org/10.1111/pcmr.13033 (2022).
16. Guo, H. et al. Establishment of an immortalized mouse dermal papilla cell strain with optimized culture strategy. *PeerJ* **6**, e4306. https://doi.org/10.7717/peerj.4306 (2018).
17. Liu, Z. et al. Endothelial cell-derived tetrahydrobiopterin prevents aortic valve calcification. *Eur. Heart J.* **43**, 1652–1664. https://doi.org/10.1093/eurheartj/ehac037 (2022).
18. Kanehisa, M., Furumichi, M., Sato, Y., Kawashima, M. & Ishiguro-Watanabe, M. KEGG for taxonomy-based analysis of pathways and genomes. *Nucleic Acids Res.* **51**, D587–D592. https://doi.org/10.1093/nar/gkac963 (2023).
19. Kanehisa, M. Toward understanding the origin and evolution of cellular organisms. *Protein Sci.* **28**, 1947–1951. https://doi.org/10.1002/pro.3715 (2019).
20. Kanehisa, M. & Goto, S. KEGG: kyoto encyclopedia of genes and genomes. *Nucleic Acids Res.* **28**, 27–30. https://doi.org/10.1093/nar/28.1.27 (2000).
21. Li, R. et al. Protein phosphatase 2A deficiency in macrophages increases foam cell formation and accelerates atherosclerotic lesion development. *Front. Cardiovasc. Med.* **8**, 745009. https://doi.org/10.3389/fcvm.2021.745009 (2021).
22. Huang, Y., Liu, M., Liu, C., Dong, N. & Chen, L. The natural product andrographolide ameliorates calcific aortic valve disease by regulating the proliferation of valve interstitial cells via the MAPK-ERK pathway. *Front. Pharmacol.* **13**, 871748. https://doi.org/10.3389/fphar.2022.871748 (2022).
23. Zhang, L. et al. Fisetin alleviated bleomycin-induced pulmonary fibrosis partly by rescuing alveolar epithelial cells from senescence. *Front. Pharmacol.* **11**, 553690. https://doi.org/10.3389/fphar.2020.553690 (2020).
24. Dutta, P. et al. KPT-330 prevents aortic valve calcification via a novel C/EBPbeta signaling pathway. *Circ. Res.* **128**, 1300–1316. https://doi.org/10.1161/CIRCRESAHA.120.318503 (2021).
25. Taniue, K., Oda, T., Hayashi, T., Okuno, M. & Akiyama, T. A member of the ETS family, EHF, and the ATPase RUVBL1 inhibit p53-mediated apoptosis. *EMBO Rep.* **12**, 682–689. https://doi.org/10.1038/embor.2011.81 (2011).

26. Muhl, L. et al. Single-cell analysis uncovers fibroblast heterogeneity and criteria for fibroblast and mural cell identification and discrimination. *Nat. Commun.* **11**, 3953. https://doi.org/10.1038/s41467-020-17740-1 (2020).
27. Rutkovskiy, A. et al. Valve interstitial cells: the key to understanding the pathophysiology of heart valve calcification. *J. Am. Heart Assoc.* https://doi.org/10.1161/JAHA.117.006339 (2017).
28. Veprintsev, D. B. et al. Core domain interactions in full-length p53 in solution. *Proc. Natl. Acad. Sci. U. S. A.* **103**, 2115–2119. https://doi.org/10.1073/pnas.0511130103 (2006).
29. Hafner, A., Bulyk, M. L., Jambhekar, A. & Lahav, G. The multiple mechanisms that regulate p53 activity and cell fate. *Nat. Rev. Mol. Cell Biol.* **20**, 199–210. https://doi.org/10.1038/s41580-019-0110-x (2019).
30. Hernandez Borrero, L. J. & El-Deiry, W. S. Tumor suppressor p53: Biology, signaling pathways, and therapeutic targeting. *Biochim. Biophys. Acta Rev. Cancer* **1876**, 188556. https://doi.org/10.1016/j.bbcan.2021.188556 (2021).
31. Maki, C. G. Oligomerization is required for p53 to be efficiently ubiquitinated by MDM2. *J. Biol. Chem.* **274**, 16531–16535. https://doi.org/10.1074/jbc.274.23.16531 (1999).
32. Kastenhuber, E. R. & Lowe, S. W. Putting p53 in context. *Cell* **170**, 1062–1078. https://doi.org/10.1016/j.cell.2017.08.028 (2017).
33. Kruse, J. P. & Gu, W. Modes of p53 regulation. *Cell* **137**, 609–622. https://doi.org/10.1016/j.cell.2009.04.050 (2009).
34. Theodoris, C. V. et al. Network-based screen in iPSC-derived cells reveals therapeutic candidate for heart valve disease. *Science.* https://doi.org/10.1126/science.abd0724 (2021).
35. Cai, Z. et al. Directed differentiation of human induced pluripotent stem cells to heart valve cells. *Circulation* **149**, 1435–1456. https://doi.org/10.1161/CIRCULATIONAHA.123.065143 (2024).
36. Li, B. & Fields, S. Identification of mutations in p53 that affect its binding to SV40 large T antigen by using the yeast two-hybrid system. *FASEB J.* **7**, 957–963. https://doi.org/10.1096/fasebj.7.10.8344494 (1993).
37. Ludlow, J. W. Interactions between SV40 large-tumor antigen and the growth suppressor proteins pRB and p53. *FASEB J.* **7**, 866–871. https://doi.org/10.1096/fasebj.7.10.8344486 (1993).
38. Aikawa, E. & Libby, P. A rock and a hard place: chiseling away at the multiple mechanisms of aortic stenosis. *Circulation* **135**, 1951–1955. https://doi.org/10.1161/CIRCULATIONAHA.117.027776 (2017).
39. Gonzalez Rodriguez, A. et al. Tumor necrosis factor-alpha promotes and exacerbates calcification in heart valve myofibroblast populations. *FASEB J.* **35**, e21382. https://doi.org/10.1096/fj.202002013RR (2021).
40. Liu, Z. et al. Long noncoding TSI attenuates aortic valve calcification by suppressing TGF-beta1-induced osteoblastic differentiation of valve interstitial cells. *Metabolism* **138**, 155337. https://doi.org/10.1016/j.metabol.2022.155337 (2023).
41. Gollmann-Tepekoylu, C. et al. Toll-like receptor 3 mediates aortic stenosis through a conserved mechanism of calcification. *Circulation* **147**, 1518–1533. https://doi.org/10.1161/CIRCULATIONAHA.122.063481 (2023).
42. Wang, X., Ali, M. S. & Lacerda, C. M. R. Osteogenesis inducers promote distinct biological responses in aortic and mitral valve interstitial cells. *J. Cell Biochem.* **120**, 11158–11171. https://doi.org/10.1002/jcb.28392 (2019).

Acknowledgements

The authors thank Dr. Geng Bingchuan for kindly reviewing and commenting this article.

Author contributions

Z.W.: Conceptualization, data curation, methodology, writing—original draft preparation. Z.R.: Visualization, writing—original draft preparation. Y.W.: Supervision, funding acquisition. N.D.: Conceptualization, funding acquisition, writing—review and editing. All the authors read and approved the final manuscript.

Funding

Funding for this project was provided by grants from the National Key R&D Program of China (2021YFA1101900), National Natural Science Foundation of China (82470423) and Hubei Provincial Natural Science Foundation Projects (JCZRYB202500142).

Declarations

Ethical approval

All experiments involving humans were conducted in accordance with the Declaration of Helsinki. The Review Board of Tongji Medical College, Huazhong University of Science and Technology, approved the research plan. (#IORG0003571).

Consent for publication

All co-authors have read the manuscript and given their approval for its final submission.

Competing interests

The authors declare no competing interests.

Additional information

Supplementary Information The online version contains supplementary material available at https://doi.org/10.1038/s41598-025-85909-z.

Correspondence and requests for materials should be addressed to N.D.